

MRI-guided Focused Ultrasound Ablation for Localized Intermediate-Risk Prostate Cancer: Early Results of a Phase II Trial

Sangeet Ghai, MD • Antonio Finelli, MD • Kateri Corr, BSc • Rosanna Chan, MRT(MR)(N) • Sarah Jokhu, HBSc • Xuan Li, PhD • Stuart McCluskey, MD, PhD • Anna Konukhova, PhD • Eugen Hlasny, MRT(MR)[†] • Theodorus H. van der Kwast, MD, PhD • Peter F. Incze, MD • Alexandre R. Zlotta, MD, PhD • Robert J. Hamilton, MD, MPH • Masoom A. Haider, MD • Walter Kucharczyk, MD • Nathan Perlis, MD, MSc

From the Joint Department of Medical Imaging (S.G., R.C., E.H., M.A.H., W.K.), Division of Urology, Department of Surgical Oncology (A.F., K.C., S.J., A.K., A.R.Z., R.J.H., N.P.), Biostatistics Department, Princess Margaret Cancer Centre (X.L.), Department of Anaesthesia (S.M.), and Department of Pathology, Laboratory Medicine Program (T.H.v.d.K.), University Health Network–Mount Sinai Hospital–Women's, College Hospital, University of Toronto, 585 University Ave, Toronto, ON, Canada M5G 2N2; and Department of Urology, Oakville Trafalgar Memorial Hospital, Toronto, Canada (P.F.I.). Received June 14, 2020; revision requested August 11; revision received October 25; accepted November 5. **Address correspondence** to S.G. (e-mail: Sangeet.Ghai@uhn.ca).

[†]Deceased.

Supported by Insightec, Ontario Research Fund, and Canadian Foundation for Innovation. The sponsors of the study had no role in data collection, data analysis, data interpretation, or writing of the report.

Conflicts of interest are listed at the end of this article.

See also the editorial by Tempany-Afdhal in this issue.

Radiology 2021; 298:695–703 • <https://doi.org/10.1148/radiol.2021202717> • Content codes: 

Background: To reduce adverse effects of whole-gland therapy, participants with localized clinically significant prostate cancer can undergo MRI-guided focal therapy.

Purpose: To explore safety and early oncologic and functional outcomes of targeted focal high-intensity focused ultrasound performed under MRI-guided focused ultrasound for intermediate-risk clinically significant prostate cancer.

Materials and Methods: In this prospective phase II trial, between February 2016 and July 2019, men with unifocal clinically significant prostate cancer visible at MRI were treated with transrectal MRI-guided focused ultrasound. The primary end point was the 5-month biopsy (last recorded in December 2019) with continuation to the 24-month follow-up projected to December 2021. Real-time ablation monitoring was performed with MR thermography. Nonperfused volume was measured at treatment completion. Periprocedural complications were recorded. Follow-up included International Prostate Symptom Score (IPSS) and International Index of Erectile Function-15 (IIEF-15) score at 6 weeks and 5 months, and multiparametric MRI and targeted biopsy of the treated area at 5 months. The generalized estimating equation model was used for statistical analysis, and the Holm method was used to adjust *P* value.

Results: Treatment was successfully completed in all 44 men, 36 with grade group (GG) 2 and eight with GG 3 disease (median age, 67 years; interquartile range [IQR], 62–70 years). No major treatment-related adverse events occurred. Forty-one of 44 participants (93%; 95% CI: 82, 98) were free of clinically significant prostate cancer (≥ 6 mm GG 1 disease or any volume \geq GG 2 disease) at the treatment site at 5-month biopsy (median, seven cores). Median IIEF-15 and IPSS scores were similar at baseline and at 5 months (IIEF-15 score at baseline, 61 [IQR, 34–67] and at 5 months, 53 [IQR, 24–65.5], *P* = .18; IPSS score at baseline, 3.5 [IQR, 1.8–7] and at 5 months, 6 [IQR, 2–7.3], *P* = .43). Larger ablations (≥ 15 cm³) compared with smaller ones were associated with a decline in IIEF-15 scores at 6 weeks (adjusted *P* < .01) and at 5 months (adjusted *P* = .07).

Conclusion: Targeted focal therapy of intermediate-risk prostate cancer performed with MRI-guided focused ultrasound ablation was safe and had encouraging early oncologic and functional outcomes.

© RSNA, 2021

Online supplemental material is available for this article

An earlier incorrect version of this article appeared online. This article was corrected on March 10, 2021

Whole-gland therapy (surgery or radiation) for prostate cancer provides excellent cancer control, but it can be associated with a significant decline in sexual and urinary function. Although prostate cancer is multifocal in 80% of patients, the natural history of the disease is predominantly determined by the index lesion, or the largest lesion that is often the highest-grade tumor in the gland (1). The index lesion is often visible at multiparametric MRI and has therefore created opportunities for focally treating the part of the gland harboring the tumor. Focal therapy

(FT), where a specific clinically significant prostate cancer (index lesion) is ablated, is a viable treatment for some localized intermediate-risk disease. The aim of FT is to eradicate clinically significant prostate cancer while minimizing morbidity associated with whole-gland treatment.

US-guided FT has been studied extensively (2–4); however, there are recent encouraging reports of MRI-guided FT (5–7). Although MRI guidance requires additional expertise, resources, and cost, it has several potential advantages. Unlike US, MRI helps to accurately localize

Abbreviations

FT = focal therapy, GG = grade group, IIEF-15 = International Index of Erectile Function-15, IPSS = International Prostate Symptom Score, IQR = interquartile range, NPV = nonperfused volume, PSA = prostate-specific antigen

Summary

Targeted focal therapy of intermediate-risk prostate cancer performed with transrectal MRI-guided focused ultrasound has encouraging early oncologic and functional outcomes.

Key Results

- In a phase II trial of 44 men with unifocal clinically significant prostate cancer visible at MRI and treated with transrectal MRI-guided focused ultrasound, 93% of men had no clinically significant prostate cancer (≥ 6 mm grade group [GG] 1 disease or any volume \geq GG 2 disease) 5 months after treatment.
- The median International Index of Erectile Function-15 (IIEF-15) score ($P = .18$) and International Prostate Symptom Score ($P = .43$) were similar at baseline and at 5 months.
- Participants with larger ablations (≥ 15 cm³ vs < 15 cm³) had a greater IIEF-15 decline at 6 weeks (adjusted $P < .01$) but a similar change at 5 months (adjusted $P = .07$).

the biopsy-proven clinically significant prostate cancer (8,9), thus allowing for better spatial resolution in all three planes for precise treatment definition. This enables a more targeted FT approach rather than a zonal ablation or hemiablation. Intuitively, smaller ablation volumes are associated with fewer adverse effects and presumably promote speedier recovery. In addition, MRI-guided FT takes advantage of MR thermography for thermal feedback during treatment (10), thus allowing for real-time power adjustment to ensure tissue ablative temperatures ($>65^{\circ}\text{C}$) are reached. After treatment, gadolinium-based contrast material is injected to assess the nonperfused volume (NPV), which provides immediate assessment of the ablated area. However, MRI underestimates the volume of disease (11,12). Thus, targeted FT templates require adequate margins beyond the visible tumor.

The three thermal energy sources studied with MRI guidance are high-intensity focused ultrasound (transrectal and transurethral routes), interstitial laser, and cryoablation (5–7,13–16). The feasibility of transrectal MRI-guided focused ultrasound FT for prostate cancer has been previously described in a phase I trial (6).

The purpose of this study was to assess safety and oncologic and functional outcomes of a targeted transrectal MRI-guided focused ultrasound treatment of intermediate-risk prostate cancer (grade group [GG] 2 and GG 3), with the primary end point at 5 months with continuation to the 24-month follow-up. Herein, we report the results of the primary end point of our phase II trial. We hypothesized that 70% of participants will respond to the treatment and will not have any residual clinically significant prostate cancer.

Materials and Methods

The study was funded by Insightec, the Ontario Research fund, and the Canadian Foundation for Innovation. The authors had full control of the data and the information submitted for pub-

lication. Five authors (S.G., N.P., K.C., S.J., and X.L.) had access to the raw data. The corresponding author had full access to all the data and had final responsibility for the decision to submit for publication.

Study Participants

Institutional review board approval was obtained for this prospective phase II trial (Appendix E1 [online]). Forty-four participants who met eligibility criteria were prospectively enrolled, following informed consent, between 2016 and 2019 at a single quaternary center. Eligible men were age 50 years or older and had intermediate-risk prostate cancer, a prostate-specific antigen (PSA) level of 20 ng/mL or less, and less than 20 mm of MRI-visible GG 2 or GG 3 disease at transrectal US-guided systematic and targeted biopsy. Participants were excluded for contraindications to MRI, intraductal carcinoma, a second site of a tumor visible at MRI, previous treatment for prostate cancer, calcification of 2 mm or greater at CT adjacent to the rectal wall or in the beam path, or if the tumor location was less than 6 cm from the rectal wall.

Pretreatment Protocol

Following referral, participants underwent MRI (Magnetom Verio 3T; Siemens) and repeat 12-core systematic biopsy with an additional two to five targeted samples from MRI-visible lesions with Artemis (version 2.0; Eigen). Participants completed questionnaires for the International Prostate Symptom Score (IPSS), International Index of Erectile Function-15 (IIEF-15), and International Consultation on Incontinence at baseline. Participants who scored a 0 for questions 2, 4, 5, and 7 on the IIEF-15 questionnaire were recorded as not sexually active.

Treatment Protocol

The Exablate 2100 Prostate (Insightec) is a transrectal MRI-guided focused ultrasound system. The 990-element phased-array transducer generates an adjustable ultrasound beam to cover a contoured region of interest within the prostate regardless of shape and location. The system helps provide a real-time therapy planning algorithm, thermal dosimetry, and closed-loop control with full MRI integration. A detailed treatment procedure with the device has been published previously (6,17). In brief, an endorectal focused ultrasound system integrated within a 1.5-T scanner (GE Signa Twinspeed HDX; GE Healthcare) was used. Procedures were performed with the participants under general anesthesia with propofol, fentanyl, and midazolam. Following bladder catheterization, the endorectal probe was inserted and filled with degassed water at 14°C for rectal cooling. A suprapubic catheter was used if the planned treatment volume included the urethra.

Spin-echo T2-weighted images and diffusion-weighted images were acquired for treatment planning. All lesions seen at baseline 3.0-T MRI were also identified with a 1.5-T scanner obtained for treatment planning. The prostate, target area, and rectal wall were manually contoured. A minimum of a 3-mm margin, and 10 mm whenever possible, beyond the visible tumor at MRI was included in the treatment planning.

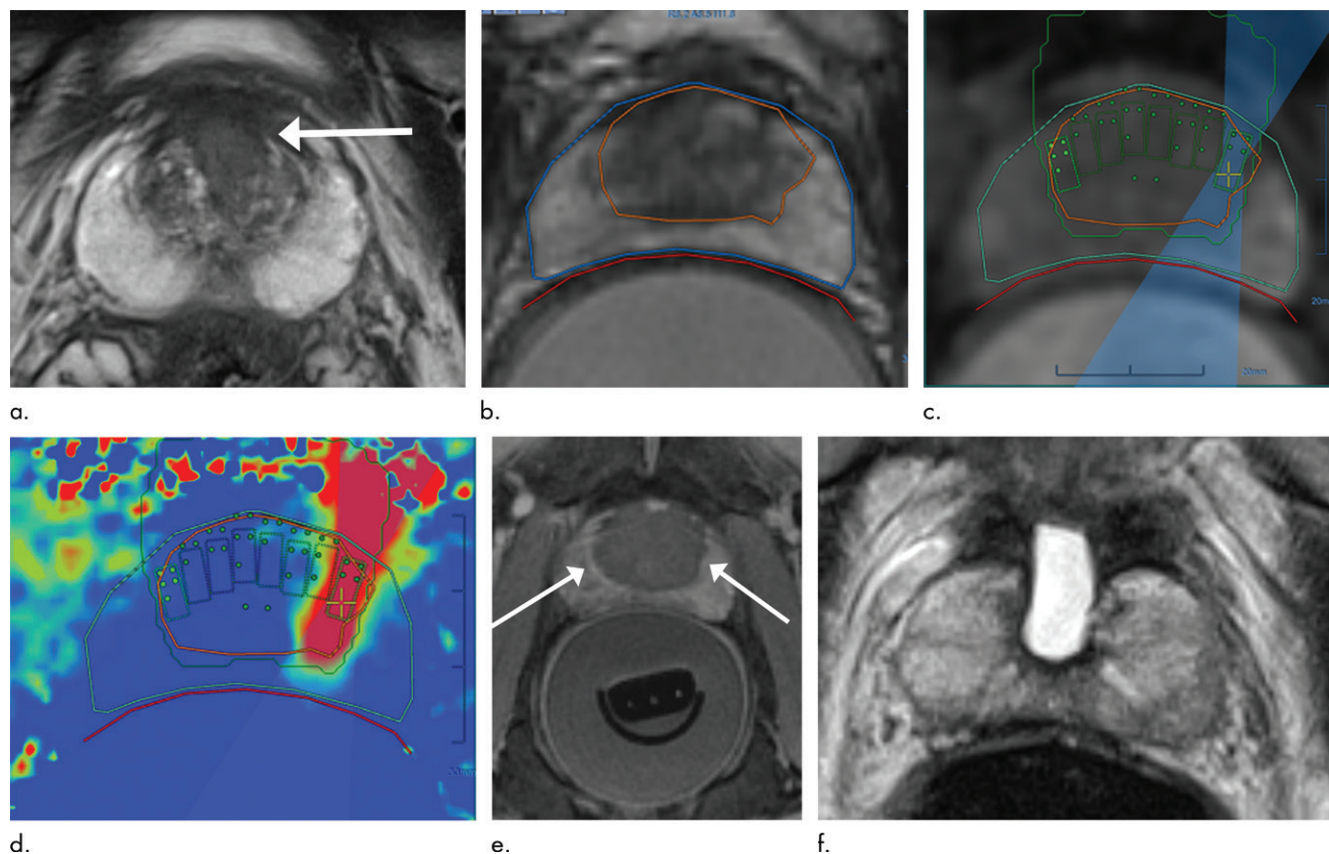


Figure 1: Images in 69-year-old man with biopsy-confirmed Gleason score 7 (3+4) prostate cancer. **(a)** Pretreatment axial T2-weighted fast spin-echo MRI scan (repetition time msec/echo time msec, 3820/97) shows tumor in midline anterior transition zone (arrow). **(b)** Intraoperative MRI scan shows contoured rectal wall (red line), prostate margin (blue outline), and region of interest (orange outline). Because the urethra was included in planned treatment volume, a suprapubic catheter was placed for continuous bladder drainage during treatment. **(c)** Intraoperative MRI scan shows focused ultrasound beam path (blue) overlaid on treatment plan. Green depicts software-generated region of expected heat deposition based on planning. Rectangles illustrate each sonication spot. **(d)** Thermal map image obtained during treatment with heat deposition color coded in red overlaid on sonication spot. **(e)** Axial gadopentetate dimeglumine-enhanced MRI scan (230/2.97) obtained immediately after treatment shows devascularized ablated volume (arrows). **(f)** Corresponding T2-weighted fast spin-echo MRI scan (3820/97) at 5 months after ablation shows complete involution of transition zone. All seven cores from treatment area margins were negative for cancer at biopsy.

The planning software (versions 6.31 and 8.0, Exablate 2100; Insightec) then computed the sonications required to treat the defined region, although this could be adjusted by the treating surgeon if desired. The acoustic power of the ultrasound device (typically 30 W) varied in conjunction with the spot location, tissue absorption, and the accumulated heat. Following a subtherapeutic verification sonication, macrosonications containing multiple spots were delivered to continuous tissue volumes within the region of treatment. Following each sonication, the system ran a new T2-weighted imaging sequence (repetition time msec/echo time msec, 3466.67/81.2; number of signals acquired, one) for generating a correlation map to baseline T2-weighted images for edge movement detection. The physician had the ability to translate the capsule contour or to ignore the movement if it was detected falsely. For lateral tumors, the ipsilateral neurovascular bundle was often heated to some degree.

Overlay of MRI thermography magnitude maps on anatomic images during treatment enabled monitoring of the ablation area. Additional single-spot nominal sonications were delivered if the desired temperature of greater than 65°C was not reached at any site. Immediate postablation

contrast-enhanced MRI (200/5) was performed to assess coverage and NPV (Figs 1, 2).

Follow-up Protocol

Participants completed questionnaires for IPSS, IIEF-15, and the International Consultation on Incontinence at follow-up clinic visits conducted at 1 week, 6 weeks, and 5 months. The PSA level was obtained at 6 weeks and 5 months, whereas multiparametric MRI and transrectal US biopsy targeted to the treatment area and to any new MRI sites was performed at 5 months. Residual disease was defined as greater than or equal to GG 2 or GG 1 cancer core length of greater than or equal to 6 mm at targeted MRI transrectal US 5-month biopsy.

Statistical Analysis

Summary statistics such as medians, interquartile ranges, frequencies, proportions, and CIs were reported to describe the participant characteristics, treatment details, quality of life, and oncologic outcomes at baseline, 6 weeks, and 5 months. Generalized estimating equation models were used to compare IIEF-15 and IPSS scores between baseline and 5 months and to evalu-

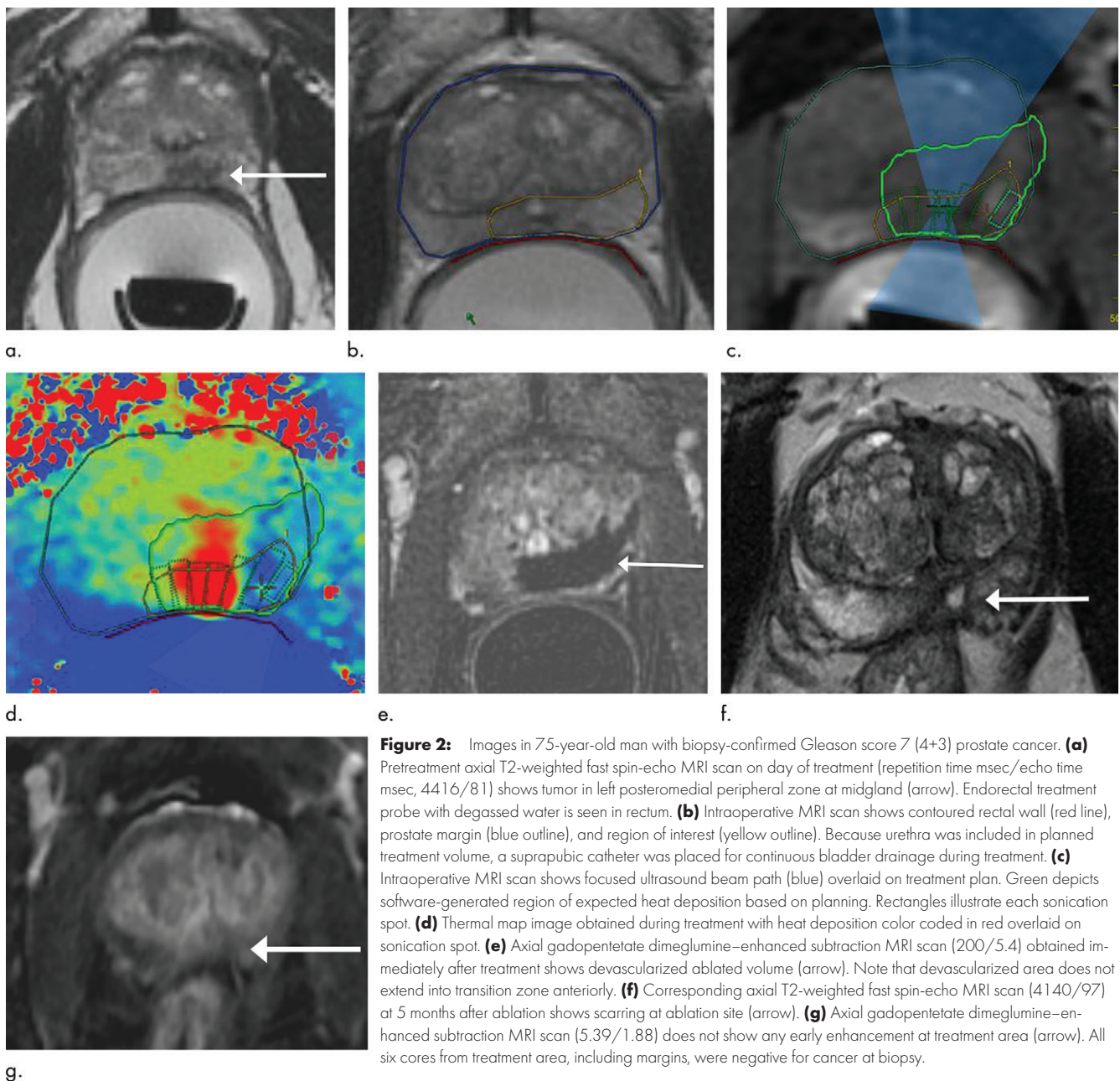


Figure 2: Images in 75-year-old man with biopsy-confirmed Gleason score 7 (4+3) prostate cancer. **(a)** Pretreatment axial T2-weighted fast spin-echo MRI scan on day of treatment (repetition time msec/echo time msec, 4416/81) shows tumor in left posteromedial peripheral zone at midgland (arrow). Endorectal treatment probe with degassed water is seen in rectum. **(b)** Intraoperative MRI scan shows contoured rectal wall (red line), prostate margin (blue outline), and region of interest (yellow outline). Because urethra was included in planned treatment volume, a suprapubic catheter was placed for continuous bladder drainage during treatment. **(c)** Intraoperative MRI scan shows focused ultrasound beam path (blue) overlaid on treatment plan. Green depicts software-generated region of expected heat deposition based on planning. Rectangles illustrate each sonication spot. **(d)** Thermal map image obtained during treatment with heat deposition color coded in red overlaid on sonication spot. **(e)** Axial gadopentetate dimeglumine-enhanced subtraction MRI scan (200/5.4) obtained immediately after treatment shows devascularized ablated volume (arrow). Note that devascularized area does not extend into transition zone anteriorly. **(f)** Corresponding axial T2-weighted fast spin-echo MRI scan (4140/97) at 5 months after ablation shows scarring at ablation site (arrow). **(g)** Axial gadopentetate dimeglumine-enhanced subtraction MRI scan (5.39/1.88) does not show any early enhancement at treatment area (arrow). All six cores from treatment area, including margins, were negative for cancer at biopsy.

ate IIEF-15 and IPSS scores across time for different groups. The Holm method was used to adjust P values from six generalized estimating equation models for IIEF-15 and from seven models for IPSS. The six IIEF-15 models involved comparisons in two treatment factors (NPV groups, neurovascular bundle, urethra included vs not included) and three clinical scenarios (between baseline and 6 weeks, between baseline and 5 months, and across three time points). Six IPSS models were similar to these in addition to evaluation of IPSS across three time points between urethra included and not included in treatment. The Holm method was performed in a stepwise way, and adjusted P values were computed according to ranks of observed P values (18). $P = .05$ was considered to indicate a statistically significant difference. Statistical analysis was performed with R software (version 3.6.1; the R Foundation for Statistical Computing).

Sample Size Calculation

The initial protocol included a sample size of 68 assuming 20% dropout and that 54 participants would provide 80% power to demonstrate 70% efficacy. Based on the 5-month and available 24-month biopsy results at the time, a sample size of 20 would have met the study hypothesis. Because one of the primary outcomes of the study was to also assess the safety of the device (grade III–V adverse events), the study was closed after 44 participants were treated.

Results

Participant Characteristics

Fifty-three men with unifocal clinically significant prostate cancer at MRI and biopsy were enrolled. There were a total

of nine screen failures, as follows: (a) three for calcification larger than 2 mm in the beam path; (b) two for hip prosthesis at the ipsilateral site of the tumor, which would have affected MRI thermography during treatment; (c) two for anterior disease more than 6 cm from the rectal wall; (d) one for previous FT treatment; and (e) one for body habitus preventing low lithotomy positioning in the magnet with an endorectal device (Fig 3).

In the end, 44 men (median age, 67 years; interquartile range [IQR], 62–70 years) were treated, 36 with GG 2 prostate cancer and eight with GG 3 disease at baseline. Clinical and treatment details are provided in Table 1. The median magnet time (MRI to recovery room) was 256 minutes, and the median ablation time was 125 minutes. Urethra, unilateral neurovascular bundle, or both were included in the treatment volume for nine, 11, and four men, respectively. No participant had bilateral neurovascular bundle included in the treatment volume.

Primary Outcomes of Safety and Targeted Biopsy

Sixteen participants experienced dysuria, which typically self-resolved by the 6-week visit. Five participants required antispasmodics for bladder spasm in the first week after treatment. Two participants had urinary retention following catheter removal and needed to be recatheterized. One man (one of 44 participants, 2%; 95% CI: 0.4, 11.8) had severe pelvic pain that persisted and reported a grade 3 adverse event at 5 months following treatment. No participant developed a recto-urethral fistula or urethral stricture or required secondary intervention.

At 5 months after ablation, three of 44 participants (7%; 95% CI: 2.4, 18.2) had residual disease at the treatment site at targeted MRI transrectal US fusion biopsy. The median number of cores from the treatment site, including margins, was seven (IQR, 6.8–7 cores; range, 6–10 cores). The median tumor dimension in the three men with residual disease was 11 mm (range, 10–14 mm), and the median NPV was 6 cm³ (range, 3.8–12.1 cm³).

In addition, new Prostate Imaging Reporting and Data System category 3 foci in the nontreated area of the gland were identified in three of 44 men at 5-month MRI. Two of these sites were negative for any disease, and one showed 2 mm of GG 1 disease at targeted biopsy. All three participants were negative for residual disease in the treatment area.

Management of Residual Disease

Among the three participants with residual disease, one was successfully treated with MRI-guided focal laser ablation for MRI-visible residual disease, whereas the other two partici-



Figure 3: Flowchart of participant enrollment. csPCa = clinically significant prostate cancer, GG = grade group, IQR = interquartile range, PCa = prostate cancer.

pants remained on active surveillance for low-volume MRI-invisible GG 2 prostate cancer (2.5 mm and 0.7 mm of disease in one of six cores and one of seven cores, respectively).

Secondary Outcomes of PSA, MRI, and Quality-of-Life Questionnaires

The median PSA level was 6.4 ng/mL (IQR, 4.3–9.6 ng/mL) at baseline and 2.4 ng/mL (IQR, 1.1–5.4 ng/mL) at 5 months after treatment. MRI scans in five of 44 participants (11%; 95% CI: 5, 24) were interpreted as suspicious or equivocal for residual disease at the treatment site, one of which showed residual disease at biopsy.

The overall IIEF-15 score at baseline and at 5 months were not significantly different (baseline, 61 [IQR, 34–67]; 5 months, 53 [IQR, 24–65.5]; $P = .18$), and neither were scores for International Index of Erectile Function-5 (or IIEF-5), intercourse satisfaction, sexual desire, orgasmic function, and overall satisfaction (Table 2). Twenty-seven men were sexually active at baseline. The median IIEF-5 score in these 27 men changed from 24 (IQR, 22–25) at baseline to 21 (IQR, 16.5–24) at 5 months. However, nine of these 27 men had at least a mild degree of new erectile dysfunction

Table 1: Clinical and Treatment Details for 44 Participants

Characteristic	Value
No. of participants	44
Gleason GG at baseline	
GG 2	36
GG 3	8
Median age (y)*	67 (62–70)
Median prostate volume (cm ³)*	40.5 (30–65)
Linear tumor size on axial image (mm)	
Median*	10 (4–19)
<10 mm	18
10–15 mm	21
>15 mm	5
Location of tumor	
Peripheral zone	35
Transition zone	9
Treatment characteristics	
Foley catheter	
No. of participants	31
Median duration (d)*	4 (3.5–5)
Suprapubic catheter	
No. of participants	19
Median duration (d)*	5 (4–7)
Median magnet time (min)*	256 (205–291.5)
Median sonication time (min)*	125 (93–159)
Median nonperfused volume (cm ³)*	9.5 (6.4–13.6)
Median ratio of nonperfused volume to prostate volume (%)*	19 (15–27)

Note.—GG = grade group.

* Numbers in parentheses are interquartile ranges.

following treatment (Table 3). Among these 27 men, 25 described erections sufficient for penetration at 5 months. Fourteen men required phosphodiesterase 5 inhibitors following FT.

All 44 men completed the IPSS questionnaires. The overall median IPSS score changed from 3.5 (IQR, 1.8–7) at baseline to 6 (IQR, 2–7.3) at 5 months ($P = .43$). The IPSS category changed in one participant from mild to moderate symptoms at 5 months. The median International Consultation on Incontinence sum score remained at 0 at baseline, 6 weeks, and 5 months.

Among the 27 participants who were sexually active at baseline, those with NPV of 15 cm³ or greater ($n = 4$) compared with those with less than 15 cm³ ($n = 23$) had a significant association with IIEF-15 score decline at 6 weeks (adjusted $P < .01$), which showed some improvement at 5 months (adjusted $P = .07$) (Fig 4). However, IIEF-15 (adjusted $P = .30$) across time was not significantly different between NPV greater than or equal to 15 cm³ and NPV less than 15 cm³. NPV of 15 cm³ or greater did not show an association with IPSS scores at 6 weeks (adjusted $P > .99$) or at 5 months (adjusted $P > .99$).

Among the 27 sexually active men at baseline, 14 had unilateral neurovascular bundle, urethra, or both included in the treatment volume. There was no significant IIEF-15 score decline in these 14 men compared with the 13

in whom the structures were spared during treatment, at 6 weeks (adjusted $P = .06$) or at 5 months after FT (adjusted $P = .16$) (Fig 5). The IIEF-15 score across time was also not significantly different between the two groups (adjusted $P = .43$). No significant difference in IPSS score change at 6 weeks (adjusted $P > .99$) and 5 months (adjusted $P > .99$) were noted when urethra, unilateral neurovascular bundle, or both ($n = 24$) were included in the treatment compared with the 20 participants in whom these structures were spared. The IPSS score across time was not significantly different between men with urethra ($n = 13$) included in the treatment volume compared with those in whom it was not included ($n = 31$) (adjusted $P > .99$).

Discussion

One of 44 participants (2%; 95% CI: 0.4, 11.8) in our study had a grade 3 adverse event at 5 months, compared with 14 of 111 participants (13%; 95% CI: 7.7, 20.1) in a multicenter hemiablation study for localized prostate cancer (19) and one of 18 (6%; 95% CI: 1.0, 25.8) following focal cryotherapy using MRI transrectal US fusion (20).

Early histologic outcomes of targeted FT with transrectal MRI-guided high-intensity focused ultrasound in our study are encouraging. Forty-one of 44 men (93%; 95% CI: 82, 98) had no residual disease at the treatment site.

Our results compare favorably to US FT, highlighting the advantages of MRI guidance and feedback (21–24). In a prospective focal high-intensity focused ultrasound trial by Guillaumier et al (2), biopsy after FT was limited to 222 of 625 men, and 40 of 222 participants had in-field recurrences (18%; 95% CI: 13.5, 23.6) versus three of 44 participants (7%; 95% CI: 2.3, 18.2) in our study. A multicenter high-intensity focused ultrasound hemiablation study (19) reported 95% without prostate cancer at the treatment site at 1 year, yet 82% of men included in the study had GG 1 disease at baseline. The MRI-visible residual disease at the treatment margin in one participant was likely from inadequate margins in the planned treatment volume, whereas in the other two, the cause of minimal residual disease may have been from heat dissipation from a small vessel. Early salvage therapy was similarly low between our trial (one participant) and the Guillaumier et al study (2), where 99% of participants avoided salvage therapy at 1 year following high-intensity focused ultrasound FT, despite 28% of participants having GG 1 disease at baseline.

In a combined analysis of 118 participants from three trials, Yap et al (25) concluded that International Index of Erectile Function scores at 1 year after ultrasound FT were not significantly different from baseline. IIEF-15 scores also initially decreased but recovered to a large extent by 5 months after FT in our study. Studies have reported that International Index of Erectile Function erectile scores continue to improve up to 12 months (23,25,26) after ablation.

The concept of FT has evolved from hemiablation or zonal ablation toward targeted ablation, including margins (27). Intuitively, larger ablation volumes should improve oncologic success but may come at a cost to the functional outcomes

Table 2: Summary of IIEF-15 Scores at Baseline, 6 Weeks, and 5 Months after Focal Therapy with MRI-guided Focused Ultrasound

Covariate	Baseline Median	6-week Median	5-month Median	P Value
IIEF-15	61 [n = 39]	32 [n = 38]	53 [n = 39]	.18
IIEF-5*	21 (1–25) [n = 44]	6.5 (1–25) [n = 42]	16 (1–25) [n = 43]	.17
OF [n = 44]*	10 (0–10)	6 (0–10)	9 (0–10)	.21
SD [n = 44]*	7 (2–10)	6 (2–10)	7 (2–10)	.21
IS [n = 44]*	10 (0–14)	0 (0–13)	8 (0–14)	.33
OS*	8 (3–10) [n = 39]	7 (2–10) [n = 38]	8 (2–10) [n = 39]	.17

Note.—P value is calculated between baseline and 5 months by using the generalized estimating equation model. IIEF-5 = International Index of Erectile Function-5, IIEF-15 = International Index of Erectile Function-15, IS = intercourse satisfaction, OF = orgasmic function, OS = overall satisfaction, SD = sexual desire.

* Numbers in parentheses are interquartile ranges. Numbers in brackets are numbers of participants.

Table 3: Summary of IIEF-5 Categories at Baseline and 5 Months after Focal Therapy in Men Who Were Sexually Active at Baseline

IIEF-5 Categories	Baseline (n = 27)	5 Months (n = 27)
No erectile dysfunction (score, 22–25)	21 (78)	12 (44)
Mild (score, 17–21)	4 (15)	8 (30)
Mild to moderate (score, 12–16)	2 (7)	2 (7)
Moderate (score, 8–11)	0 (0)	1 (4)
Severe (score, 5–7)	0 (0)	1 (4)
Not applicable (score, 0–4)	0 (0)	3 (11)

Note.—Data are numbers of men, with percentages in parentheses. IIEF-5 = International Index of Erectile Function-5.

(26). Targeted ablation, without compromising oncologic outcomes, can therefore be best obtained when the tumor is visible during therapy, and real-time closed-loop feedback is available such that the treatment volume and energy magnitude can be altered if needed. FT with MRI allows for all of these advantages and hence has the potential of delivering the best FT outcomes, from both an oncologic and functional standpoint. Our results show that ablation volumes of 15 cm³ or greater resulted in a significant decrease in erectile function at 6 weeks, with some improvement over time. This may imply that tissue preservation leads to functional preservation. However, given the small cohort with larger ablation volumes in our study, this would need to be validated in larger multicenter trials.

The small number of participants with residual disease following treatment did not allow us to test associations of PSA levels or MRI with residual disease. However, studies have shown that PSA is not reliable to detect early recurrent or residual disease following FT (28). There is a variable reduction in prostate volume after FT that may account for a decrease in PSA (29). This makes PSA particularly unreliable in the early follow-up period after FT. Once a nadir is reached, PSA velocity may be a helpful marker in detecting recurrent disease at late follow-up (30). MRI has been shown to perform better than PSA measurements in helping to detect residual disease after FT (31,32) and is recommended in surveillance by expert consensus panels (33).

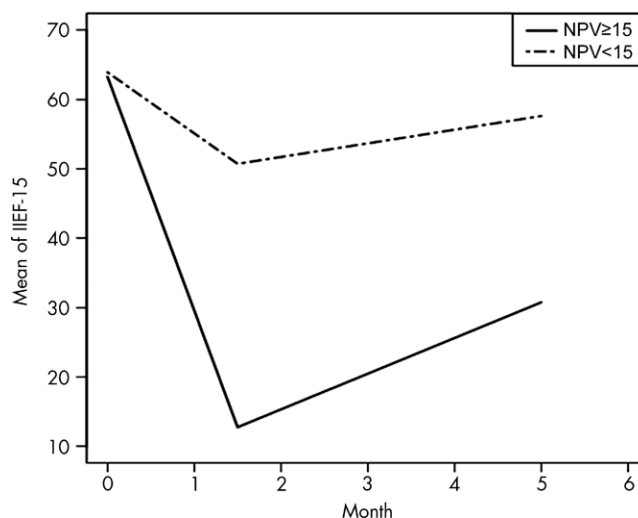


Figure 4: Sexual function results after MRI-guided focused ultrasound for unifocal localized intermediate-risk prostate cancer, measured with International Index of Erectile Function-15 (IIEF-15) questionnaire. Graph obtained with generalized estimating equation statistical model shows mean of IIEF-15 scores across time between groups of treatments with nonperfused volume (NPV) of less than 15 cm³ (n = 23) and 15 cm³ or greater (n = 4) among participants who were sexually active at baseline (adjusted P = .30). Mean ± standard deviation of NPV less than 15 cm³ was 63.9 ± 8.3 at baseline, 12.8 ± 5.6 at 6 weeks, and 30.8 ± 20.1 at 5 months. Mean ± standard deviation of NPV greater than 15 cm³ was 63.2 ± 6.7 at baseline, 50.7 ± 17.7 at 6 weeks, and 57.6 ± 15.2 at 5 months.

MRI helped identify disease as a focus of early enhancement (34) in one of three men with residual disease in our study. The two MRI-invisible sites of minimal-volume residual disease were identified at extended sampling (median, seven cores), which otherwise may have gone undetected at multiparametric MRI or biopsy. Our findings support the expert panels' recommendation that biopsy after FT should include four to six targeted cores from the ablation zone, including margins, to account for fibrosis-related gland deformity and possible fusion misregistration (33).

MRI guidance for FT requires additional resources and time, leading to increased costs. The median magnet time was 256 minutes in our trial compared with 144.5 and 135 minutes anesthesia time reported for targeted high-intensity focused ultrasound (22,23). However, if further studies confirm the oncologic

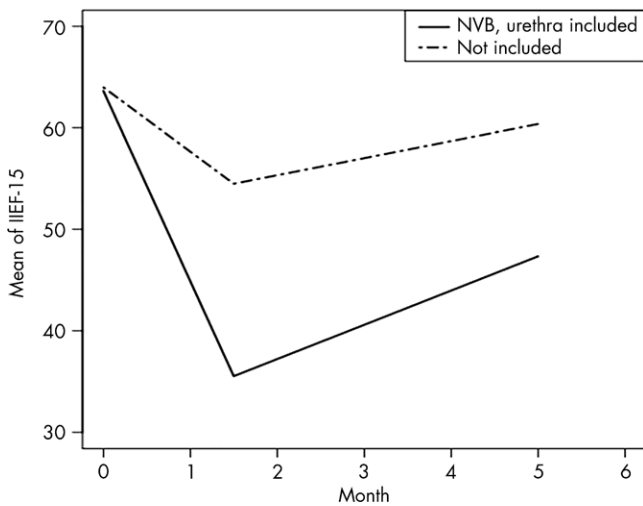


Figure 5: Sexual function results after MRI-guided focused ultrasound for unifocal localized intermediate-risk prostate cancer, measured with International Index of Erectile Function-15 (IIEF-15) questionnaire. Graph obtained with generalized estimating equation statistical model shows mean of IIEF-15 scores across time between groups of participants undergoing treatments where unilateral neurovascular bundle (NVB), urethra, or both were included in the treatment volume ($n = 14$) versus those participants in whom these structures were spared ($n = 13$), among men who were sexually active at baseline (adjusted $P > .99$). Mean \pm standard deviation of NVB, urethra included, was 63.6 ± 6.9 at baseline, 35.5 ± 22.8 at 6 weeks, and 47.4 ± 22.6 at 5 months. Mean \pm standard deviation of NVB, urethra not included, was 64 ± 9.3 at baseline, 54.4 ± 15.8 at 6 weeks, and 60.4 ± 8.8 at 5 months.

and functional benefit of MRI-guided FT, then the costs may be justified.

Our study had several limitations. First, because we focused on early outcomes, the follow-up period is short. Twenty-four participants have reached 2-year follow-up, and one other participant has clinically significant prostate cancer (not MRI visible and continues on active surveillance). Second, our population size was small and limited to men with unifocal clinically significant prostate cancer, which may not be generalizable to many men with prostate cancer. Third, 5-month sampling was restricted to the treatment area and additional sites if questioned at MRI. Because men had two systematic biopsies for inclusion, we did not believe there was value in adding systematic biopsy to the 5-month MRI examination and extended treatment area biopsy. Questions around de novo, persistent, and recurrent prostate cancer will be explored with the mandated 24-month systematic and targeted biopsies.

In conclusion, targeted focal therapy of intermediate-risk prostate cancer performed with transrectal MRI-guided focused ultrasound has encouraging early oncologic outcomes and a low rate of genitourinary adverse effects.

Author contributions: Guarantors of integrity of entire study, S.G., A.F., S.M.; study concepts/study design or data acquisition or data analysis/interpretation, all authors; manuscript drafting or manuscript revision for important intellectual content, all authors; approval of final version of submitted manuscript, all authors; agrees to ensure any questions related to the work are appropriately resolved, all authors; literature research, S.G., S.J., X.L., T.H.v.d.K., N.P.; clinical studies, S.G., A.F., K.C., R.C., S.J., X.L., A.K., E.H., T.H.v.d.K., P.F.I., A.R.Z., W.K., N.P.; experimental studies, R.C., X.L., N.P.; statistical analysis, S.J., X.L., N.P.; and manuscript editing, S.G., A.F., K.C., R.C., X.L., A.K., T.H.v.d.K., P.F.I., A.R.Z., R.J.H., M.A.H., W.K., N.P.

Disclosures of Conflicts of Interest: S.G. Activities related to the present article: institution received grants from Insightec Ltd, Ontario Research Fund, and Canadian Foundation for Innovation. Activities not related to the present article: received reimbursement for travel, accommodations, and meeting expenses from Insightec Ltd. Other relationships: disclosed no relevant relationships. A.F. Activities related to the present article: institution received grant. Activities not related to the present article: is a consultant for Astellas, Janssen, Abbvie, Bayer, Hoffman-La Roche, Amgen, Sanofi Pasteur, Ipsen, Ferring, and Tesaro. Other relationships: disclosed no relevant relationships. K.C. Activities related to the present article: institution received grants from Insightec Ltd, Ontario Research Fund, and Canadian Foundation for Innovation. Activities not related to the present article: disclosed no relevant relationships. Other relationships: disclosed no relevant relationships. R.C. Activities related to the present article: institution received grants from Insightec Ltd, Ontario Research Fund, and Canadian Foundation for Innovation. Activities not related to the present article: disclosed no relevant relationships. Other relationships: disclosed no relevant relationships. S.J. Activities related to the present article: institution received grants from Insightec Ltd, Ontario Research Fund, and Canadian Foundation for Innovation. Activities not related to the present article: disclosed no relevant relationships. Other relationships: disclosed no relevant relationships. X.L. disclosed no relevant relationships. S.M. disclosed no relevant relationships. A.K. disclosed no relevant relationships. A.K. disclosed no relevant relationships. E.H. disclosed no relevant relationships. T.H.v.d.K. Activities related to the present article: disclosed no relevant relationships. Activities not related to the present article: is a consultant for Janssen Pharmaceuticals; has grants/grants pending. Other relationships: disclosed no relevant relationships. P.F.I. disclosed no relevant relationships. A.R.Z. disclosed no relevant relationships. R.J.H. Activities related to the present article: disclosed no relevant relationships. Activities not related to the present article: serves on the advisory boards of Abbvie, Astellas, Janssen, and Bayer; received payment for lectures, including service on speakers bureaus, from Bayer and Astellas; received reimbursement for travel, accommodations, and meeting expenses from Sanofi. Other relationships: disclosed no relevant relationships. M.A.H. disclosed no relevant relationships. W.K. disclosed no relevant relationships. N.P. Activities related to the present article: institution received funding from Insightec Ltd, Ontario Research Fund, and Canadian Foundation for Innovation. Activities not related to the present article: serves on the advisory boards of Terserra, Abbvie, and Focal Healthcare; received payment for lectures, including service on speakers bureaus, from Abbvie; received reimbursement for travel, accommodations, and meeting expenses from Spectracore. Other relationships: disclosed no relevant relationships.

References

- Karavidakis M, Winkler M, Abel P, Livni N, Beckley I, Ahmed HU. Histological characteristics of the index lesion in whole-mount radical prostatectomy specimens: implications for focal therapy. *Prostate Cancer Prostatic Dis* 2011;14(1):46–52.
- Guillaumier S, Peters M, Arya M, et al. A Multicenter Study of 5-year Outcomes Following Focal Therapy in Treating Clinically Significant Nonmetastatic Prostate Cancer. *Eur Urol* 2018;74(4):422–429.
- Stabile A, Orczyk C, Hosking-Jervis F, et al. Medium-term oncological outcomes in a large cohort of men treated with either focal or hemi-ablation using high-intensity focused ultrasonography for primary localized prostate cancer. *BJU Int* 2019;124(3):431–440.
- Tay KJ, Polascik TJ. Focal Cryotherapy for Localized Prostate Cancer. *Arch Esp Urol* 2016;69(6):317–326.
- Eggerer SE, Yousuf A, Watson S, Wang S, Oto A. Phase II Evaluation of Magnetic Resonance Imaging Guided Focal Laser Ablation of Prostate Cancer. *J Urol* 2016;196(6):1670–1675.
- Ghai S, Perlis N, Lindner U, et al. Magnetic resonance guided focused high frequency ultrasound ablation for focal therapy in prostate cancer - phase 1 trial. *Eur Radiol* 2018;28(10):4281–4287.
- Chin JL, Billia M, Relle J, et al. Magnetic Resonance Imaging-Guided Transurethral Ultrasound Ablation of Prostate Tissue in Patients with Localized Prostate Cancer: A Prospective Phase 1 Clinical Trial. *Eur Urol* 2016;70(3):447–455.
- Siddiqui MM, Rais-Bahrami S, Turkbey B, et al. Comparison of MR/ultrasound fusion-guided biopsy with ultrasound-guided biopsy for the diagnosis of prostate cancer. *JAMA* 2015;313(4):390–397.
- Kasivisvanathan V, Rannikko AS, Borghi M, et al. MRI-Targeted or Standard Biopsy for Prostate-Cancer Diagnosis. *N Engl J Med* 2018;378(19):1767–1777.
- Odén H, Parker DL. Magnetic resonance thermometry and its biological applications - Physical principles and practical considerations. *Prog Nucl Magn Reson Spectrosc* 2019;110:34–61.
- Le Nobin J, Rosenkrantz AB, Villers A, et al. Image Guided Focal Therapy for Magnetic Resonance Imaging Visible Prostate Cancer: Defining a 3-Dimensional Treatment Margin Based on Magnetic Resonance Imaging Histology Co-Registration Analysis. *J Urol* 2015;194(2):364–370.
- Priester A, Natarajan S, Khoshnoodi P, et al. Magnetic Resonance Imaging Underestimation of Prostate Cancer Geometry: Use of Patient Specific Molds to Correlate Images with Whole Mount Pathology. *J Urol* 2017;197(2):320–326.
- Mathew MS, Oto A. MR Imaging-Guided Focal Therapies of Prostate Cancer. *Magn Reson Imaging Clin N Am* 2019;27(1):131–138.
- Overduin CG, Bomers JG, Jenniskens SF, et al. T1-weighted MR image contrast around a cryoablation iceball: a phantom study and initial comparison with in vivo findings. *Med Phys* 2014;41(11):112301.

15. Oto A, Sethi I, Karczmar G, et al. MR imaging-guided focal laser ablation for prostate cancer: phase I trial. *Radiology* 2013;267(3):932–940.
16. Lindner U, Lawrentschuk N, Weersink RA, et al. Focal laser ablation for prostate cancer followed by radical prostatectomy: validation of focal therapy and imaging accuracy. *Eur Urol* 2010;57(6):1111–1114.
17. Ghai S, Louis AS, Van Vliet M, et al. Real-Time MRI-Guided Focused Ultrasound for Focal Therapy of Locally Confined Low-Risk Prostate Cancer: Feasibility and Preliminary Outcomes. *AJR Am J Roentgenol* 2015;205(2):W177–W184.
18. Holm S. A simple sequentially rejective multiple test procedure. *Scand J Stat* 1979;6:65–70.
19. Rischmann P, Gelet A, Riche B, et al. Focal High Intensity Focused Ultrasound of Unilateral Localized Prostate Cancer: A Prospective Multicentric Hemiablation Study of 111 Patients. *Eur Urol* 2017;71(2):267–273.
20. Valerio M, Shah TT, Shah P, et al. Magnetic resonance imaging-transrectal ultrasound fusion focal cryotherapy of the prostate: A prospective development study. *Urol Oncol* 2017;35(4):150.e1–150.e7.
21. Shah TT, Kasivisvanathan V, Jameson C, Freeman A, Emberton M, Ahmed HU. Histological outcomes after focal high-intensity focused ultrasound and cryotherapy. *World J Urol* 2015;33(7):955–964.
22. Ahmed HU, Hindley RG, Dickinson L, et al. Focal therapy for localised unifocal and multifocal prostate cancer: a prospective development study. *Lancet Oncol* 2012;13(6):622–632.
23. Ahmed HU, Dickinson L, Charman S, et al. Focal Ablation Targeted to the Index Lesion in Multifocal Localised Prostate Cancer: a Prospective Development Study. *Eur Urol* 2015;68(6):927–936.
24. Bass R, Fleshner N, Finelli A, Barkin J, Zhang L, Klotz L. Oncologic and Functional Outcomes of Partial Gland Ablation with High Intensity Focused Ultrasound for Localized Prostate Cancer. *J Urol* 2019;201(1):113–119.
25. Yap T, Ahmed HU, Hindley RG, et al. The Effects of Focal Therapy for Prostate Cancer on Sexual Function: A Combined Analysis of Three Prospective Trials. *Eur Urol* 2016;69(5):844–851.
26. Faure Walker NA, Norris JM, Shah TT, et al. A comparison of time taken to return to baseline erectile function following focal and whole gland ablative therapies for localized prostate cancer: A systematic review. *Urol Oncol* 2018;36(2):67–76.
27. Lebastchi AH, George AK, Polascik TJ, et al. Standardized Nomenclature and Surveillance Methodologies After Focal Therapy and Partial Gland Ablation for Localized Prostate Cancer: An International Multidisciplinary Consensus. *Eur Urol* 2020;78(3):371–378.
28. Barret E, Harvey-Bryan KA, Sanchez-Salas R, Rozet F, Galiano M, Cathelineau X. How to diagnose and treat focal therapy failure and recurrence? *Curr Opin Urol* 2014;24(3):241–246.
29. Bozzini G, Colin P, Nevoux P, Villers A, Mordon S, Betrouni N. Focal therapy of prostate cancer: energies and procedures. *Urol Oncol* 2013;31(2):155–167.
30. Huber PM, Afzal N, Arya M, et al. Prostate Specific Antigen Criteria to Diagnose Failure of Cancer Control following Focal Therapy of Nonmetastatic Prostate Cancer Using High Intensity Focused Ultrasound. *J Urol* 2020;203(4):734–742.
31. Dickinson L, Ahmed HU, Hindley RG, et al. Prostate-specific antigen vs. magnetic resonance imaging parameters for assessing oncological outcomes after high intensity-focused ultrasound focal therapy for localized prostate cancer. *Urol Oncol* 2017;35(1):30.e9–30.e15.
32. Punwani S, Emberton M, Walkden M, et al. Prostatic cancer surveillance following whole-gland high-intensity focused ultrasound: comparison of MRI and prostate-specific antigen for detection of residual or recurrent disease. *Br J Radiol* 2012;85(1014):720–728.
33. Muller BG, van den Bos W, Brausi M, et al. Follow-up modalities in focal therapy for prostate cancer: results from a Delphi consensus project. *World J Urol* 2015;33(10):1503–1509.
34. Felker ER, Raman SS, Lu DSK, et al. Utility of Multiparametric MRI for Predicting Residual Clinically Significant Prostate Cancer After Focal Laser Ablation. *AJR Am J Roentgenol* 2019;213(6):1253–1258.

Erratum

Originally published in:

Radiology 2021;298(3):695–703

<https://pubs.rsna.org/doi/10.1148/radiol.2021202717>

MRI-guided Focused Ultrasound Ablation for Localized Intermediate-Risk Prostate Cancer: Early Results of a Phase II Trial

Sangeet Ghai, Antonio Finelli, Kateri Corr, Rosanna Chan, Sarah Jokhu, Xuan Li, Stuart McCluskey, Anna

Konukhova, Eugen Hlasny, Theodorus H. van der Kwast, Peter F. Incze, Alexandre R. Zlotta, Robert J. Hamilton, Masoom A. Haider, Walter Kucharczyk, Nathan Perli

Erratum in:

<https://pubs.rsna.org/doi/10.1148/radiol.2021219007>

In Table 2, the IIEF-15 5-month median value should appear as follows: **53**.